

Supplementary Information

Identifying Descriptor of Governing NO Oxidation on Mullite Sm(Y, Tb, Gd, Lu)Mn₂O₅ for Diesel Exhaust Cleaning

Hao-Bo Li¹, Wei-Hua Wang¹, Xinyu Qian¹, Yahui Cheng¹, Xinjian Xie², Jieyu Liu¹, Shuhui Sun³, Jigang Zhou⁴, Yongfeng Hu⁴, Jianping Xu⁵, Lan Li⁵, Yan Zhang⁶, Xiwen Du⁶, Kuanghong Gao⁷, Zhiqing Li⁷, Cui Zhang⁸, Shudong Wang⁹, Haijun Chen⁹, Yidong Zhao¹⁰, Feng Lu^{1,†}, Weichao Wang^{1,†}, Hui Liu¹

¹*Nankai University, College of Electronic Information and Optical Engineering, Tianjin, China, 300071*

²*School of Materials Science and Engineering, Hebei University of Technology, Tianjin, China, 300130*

³*Institut National de la Recherche Scientifique, Qu ébec, Canada J3X 1S2*

⁴*Canadian Light Source, Saskatoon, Canada, S7N 2V3*

⁵*Tianjin University of Technology, College of Science, Tianjin, China, 300384*

⁶*Tianjin University, School of Materials Science and Engineering, Tianjin, China, 300072*

⁷*Tianjin University, Department of Physics, Tianjin, China, 300072*

⁸*Nankai University, College of Chemistry, Tianjin, China, 300071.*

⁹*Dalian Institute of Chemical Physics, Chinese Academy of Sciences, Dalian, China, 116023.*

¹⁰*Beijing Synchrotron Radiation Facility, Chinese Academy of Sciences, Beijing, China, 100049.*

†To whom correspondence should be addressed.

Email: lufeng@nankai.edu.cn; weichaowang@nankai.edu.cn

Index	Page
Supplementary methods	3-5
Figure S1-S5	6-7
Table S1	8
Reference	9

Supplementary methods

Hydrothermal synthesis of $Sm(Tb, Y)Mn_2O_5$. All the $Sm(Y, Tb)Mn_2O_5$ nanoparticles were synthesized by hydrothermal method. Rare-earth nitrate, $Mn(CH_3CO_2)_2 \cdot 4H_2O$ and $KMnO_4$ (all 99.98%, Aladdin) were dissolved in 25 ml deionized water in a molar ratio of 5:7:3 and stirred for 30 minutes. Then the NaOH (99.98%, Aladdin) solution of 5 M was added slowly and the mixture was stirred for another 10 minutes. The precursor was transferred to a 100 ml stainless steel Teflon-lined autoclave which was then filled to 60% of its capacity. The hydrothermal treatment was processed under 200 °C for 12 hours. After the autoclave was cooled down to the room temperature, the product was filtered and washed by deionized water and 1% HNO_3 for 3~5 times. The precipitant was dried at 80 °C for 4 hours. To determine the phase purity, all the samples were characterized by X-ray diffraction (Rigaku Corporation, D/max-2500). The morphology of the nanoparticles was obtained from transmission electron microscope (TEM) by TECNAI F30.

X-ray diffraction spectra. The X-ray diffraction (XRD) spectra is plotted in Figure S1 and the pure mullite crystalline are in orthorhombic phases with space group of $Pbam$.

BET surface area measurement. The BET surface areas of samples were determined from N_2 adsorption-desorption experiments, which was carried out at -196 °C on

Microporous instrument Tristar 3000. The samples were outgassed for 10 hours at 300 °C to remove any moisture or adsorbed contaminants that may have been present on their surface. The specific surface area (SBET) was calculated using the Brunauer-Emmett-Teller (BET) method, which was presented in Tristar 3000 apparatus.

Catalytic characterization. All the samples are in powder form and the catalytic measurement was carried out using a flow through powder reactor system equipped with a Fourier Transform Infrared (FT-IR) spectrometer (Nicolet 6700) with a gas sampling cell at atmospheric pressure. The samples weight was 0.6 g and the total flow rate was 200 sccm, which consists of 450 ppmv NO and 10% O₂/He. The NO conversion was obtained by calculating the molar ratio between the produced NO₂ to the entered NO.

DFT calculations of bulk mullite oxides. The Sm(Y, Tb)Mn₂O₅ system belongs to orthorhombic space group *Pbam* containing two different types of Mn-O ligand field of octahedral and square pyramid as shown in Figure S2. In fact neutron and x-ray diffraction studies claim that the actual symmetry group is *Pb2₁m*, which results in complicated magnetic structures and macroscopic electric polarization along the *b* direction¹⁻³. In order to fit the magnetic period, the calculated structure of Sm(Y, Tb)Mn₂O₅ contains a 2×1×1 unit cell which is in line with other collinear calculations on mullite⁴⁻⁶. Along the *b* direction, the spin ordering of the Mn ions in Sm(Y,

Tb)Mn₂O₅ could be schematically represented as a chain of Mn_{pyr}[↑] – O_{bulk} – Mn_{oct}[↑] – O_{bulk} – Mn_{pyr}[↓] as shown in Figure S2. The Mn_{pyr}[↑] – O_{bulk} – Mn_{oct}[↑] part of the chain plays key role in governing the O* releasing difficulty. The spin-splitting *d*-band alignment is verified by investigating the partial charge distribution within the certain range of the projected density of states of Mn ions. As the *d*-orbitals expand, the *d*-orbitals overlap with each other, thus the regions contributed by certain *d*-orbitals are labeled in Figure S3 to identify the *d*-orbitals sequence.

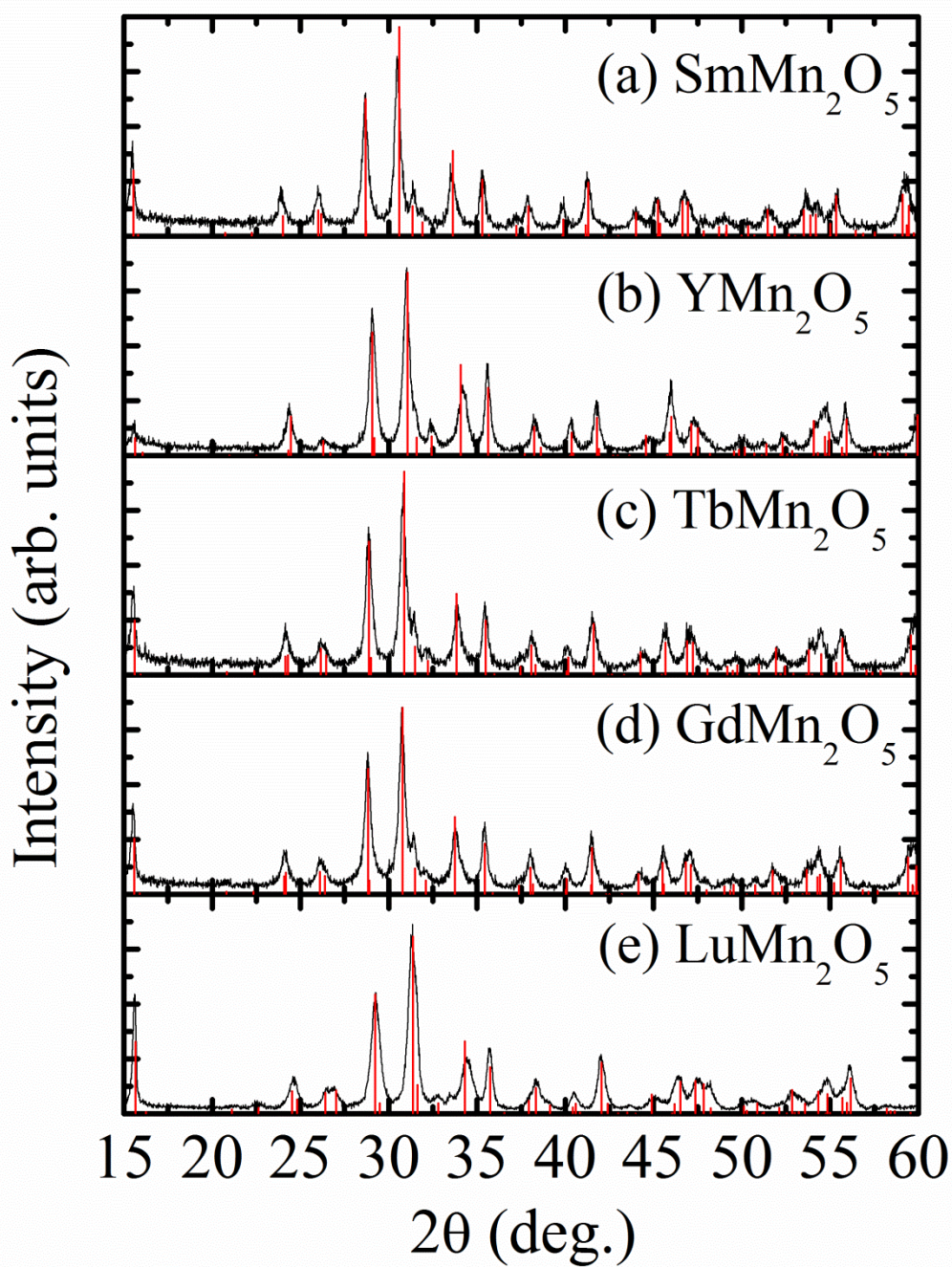


Figure S1. The XRD spectra of AMn_2O_5 ($A=\text{Sm}, \text{Y}, \text{Tb}, \text{Gd}, \text{Lu}$). The red line are the standard peaks.

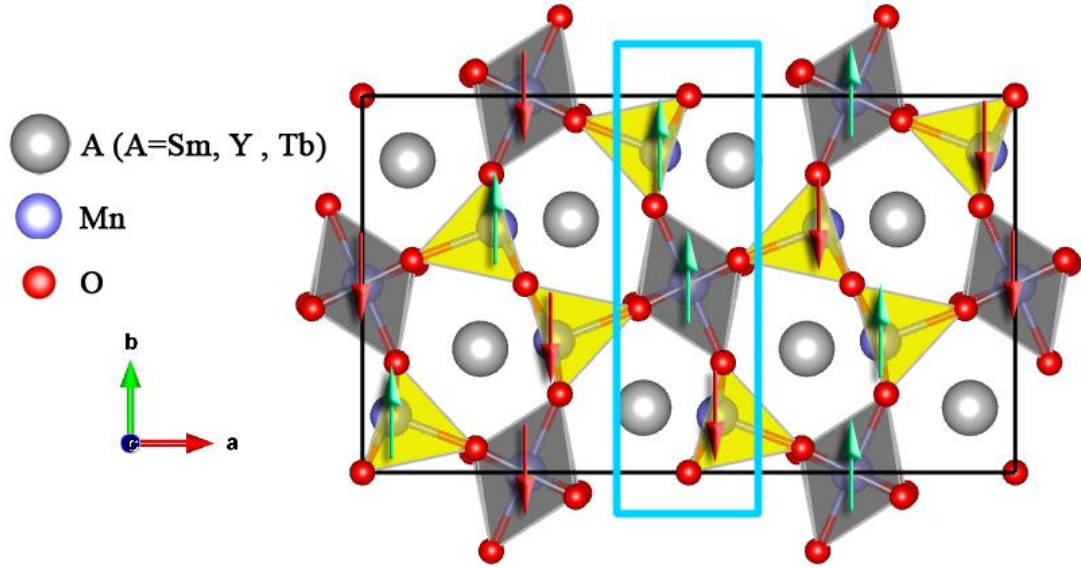


Figure S2. (Color online) The $2 \times 1 \times 1$ unit cell of $\text{Sm}(\text{Y}, \text{Tb})\text{Mn}_2\text{O}_5$. The two types of ligand field: octahedral and square pyramid are labeled by grey and yellow area, respectively. The arrows represent the spin configuration in collinear approximation in calculations. The blue square denotes the $\text{Mn}_{\text{pyr}}^{\uparrow} - \text{O}_{\text{bulk}} - \text{Mn}_{\text{oct}}^{\uparrow} - \text{O}_{\text{bulk}} - \text{Mn}_{\text{pyr}}^{\downarrow}$ chain.

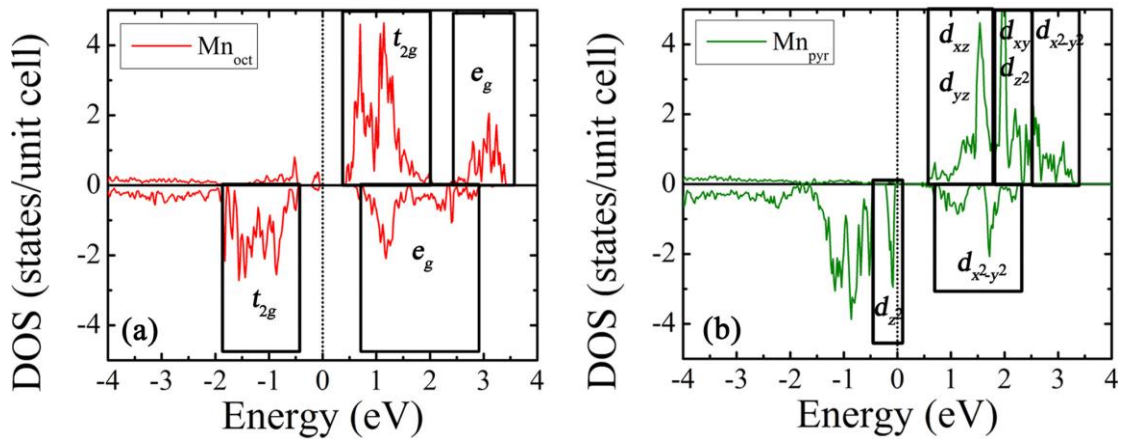


Figure S3. (Color online) Spin-polarized projected density of states (PDOS). (a), PDOS of $\text{Mn}_{\text{oct}}-3d$. (b), PDOS of $\text{Mn}_{\text{pyr}}-3d$. Regions contributed by different orbitals are labeled.

Table S1: The BET surface area of different samples.

Sample	BET surface area (m²/g)
SmMn ₂ O ₅	54.3
YMn ₂ O ₅	55.6
TbMn ₂ O ₅	52.1
LuMn ₂ O ₅	54.4
GdMn ₂ O ₅	68.0

Reference

- ¹ I. Kagomiya, S. Mastumoto, K. Kohn, Y. Fukuda, T. Shoubu, H. Kimura, Y. Noda, and N. Ikeda, *Ferroelectrics* **286**, 167 (2003).
- ² L. C. Chapon, G. R. Blake, M. J. Gutmann, S. Park, N. Hur, P. G. Radaelli, S-W. Cheong, *Phys. Rev. Lett.* **93**, 177402. (2004).
- ³ J. A. Alonso, M. T. Casais, M. J. Martínez-Lopey, J. L. Martínez, and M. T. Fernández-Dáz, *J. Phys.: Condens. Matter* **9**, 8515 (1997).
- ⁴ C. Wang, G.-C. Guo and L. He, *Phys. Rev. Lett.* **99**, 177202 (2007).
- ⁵ G. Giovannetti and J. Brink, *Phys. Rev. Lett.* **100**, 227603 (2008).
- ⁶ T. -R. Chang, H.-T. Jeng, C.-Y. Ren and C.-S. Hsue, *Phys. Rev. B* **84**, 024421. (2011).